NASA Technical Memorandum 104097

EFFECTS OF NOZZLE EXIT GEOMETRY AND PRESSURE RATIO ON PLUME SHAPE FOR NOZZLES EXHAUSTING INTO QUIESCENT AIR

W. I. Scallion

May 1991

NASA
National Aeronautics and Space Administration

Langley Research Center
Hampton, Virginia 23665-5225

EFFECTS OF NOZZLE EXIT GEOMETRY AND PRESSURE RATIO ON PLUME SHAPE FOR NOZZLES EXHAUSTING INTO QUIESCENT AIR

BY

W. I. Scallion

ABSTRACT

As part of an RCS-flow field interaction study, tests were performed in the Langley Nozzle Test Chamber on a series of nozzles to determine the qualitative effects of varying nozzle exit geometry and exit-to-ambient pressure ratio on the plume shape. The nozzles, which had circular throats and circular, elliptical, and oval exit cross sections, had design Mach numbers ranging from 3.14 to 3.87. They were supplied with dry unheated air at pressures up to 200 psi and exhausted into quiescent air. The plume shapes were photographically recorded from schlieren images and were compared to predicted axisymmetric plume shapes. These tests demonstrated that, at exit-to-ambient pressure ratios of 30 and above, plumes equivalent in size and shape to the circular nozzle plumes could be generated by the non-circular nozzles with lower chamber pressures and mass flow rates; but at exit pressure ratios less than 30 the non-circular nozzles generated much smaller plumes than the circular nozzle at comparable exit pressure ratios.

SUMMARY

Tests were conducted in quiescent air on a series of nozzles having circular throats and circular, elliptical, and oval exit cross sections to determine the qualitative effects of the exit shape on the plume shape at several exit-to-ambient pressure ratios. The circular nozzle and two of the non-circular nozzles had the same circular throat diameters, while the third non-circular nozzle throat area was one-half the others. The exit areas of the non-circular nozzles were approximately one-half the exit area of the circular nozzle. The plume shapes were recorded on schlieren photographs and were compared to each other and to predicted axisymmetric shapes on the basis of similar exit-to-ambient pressure ratios. At the lower exit pressure ratios, the non-circular nozzle plumes were smaller than the circular nozzle plumes, but at exit pressure ratios of 30 and above, the non-circular nozzles generated plumes of comparable shape and size, and these plumes were also generated with lower mass flow rates than were the circular nozzle plumes.

INTRODUCTION

Simulating the exhaust of a rocket motor in conventional supersonic and hypersonic wind tunnels is challenging, primarily because of the requirement for simultaneous scaling of the model rocket parameters to tunnel free-stream conditions, even when the model rocket is an exact scaled duplicate with reacting exhaust flows. Because of these difficulties, many studies involving rocket exhaust effects have been conducted with non-reacting, unheated gases such as dry air or nitrogen (Reference 1). In cases where the rocket motors encounter a wide range of flight

conditions, it is desirable to match the ratios of the rocket model mass-flow, momentum, and exit pressure to free-stream conditions with those of the actual flight conditions. The aforementioned challenges in accomplishing this become apparent, when for a given scaled model nozzle geometry, calculations of the chamber pressures required to meet the desired conditions for one parameter result in mismatched values for the other two parameters. The largest mismatch is between the two flow parameters (mass flow and momentum) and the exit pressure ratio. For example, calculations of the model nozzle chamber pressures required to match the flight exit-to-ambient pressure ratios (governing the exit plume shape) result in model momentum and mass-flow ratios that in most cases greatly exceed the corresponding flight values. One way to partially circumvent this is to reduce the model nozzle exit area (and consequently reduce the exit Mach number), and therefore, increase the exit-to-ambient pressure ratios with correspondingly larger exhaust plumes, without increasing the mass flow; however, it is necessary to maintain the nozzle exit plane dimension perpendicular to the local free stream flow to scale. This can be done by reducing the nozzle exit dimension parallel to the free stream flow to effectively reduce the exit area, thereby creating a non-circular exit.

As the initial phase of an effort to design a set of nozzles for wind-wind-tunnel tests of a spacecraft reaction control system (RCS), a qualitative study was conducted to determine the effect of varying the nozzle shape at the exit plane and the nozzle exit-to-ambient pressure ratio on the shape of the plume in quiescent air. Since in actual flight the nozzles were to exhaust transversely into a moving stream, it was believed that exit plume shape was an important factor in reproducing the

interactions between the rocket exhaust and the flow field. The tests reported herein were conducted in the Langley Nozzle Test Chamber in quiescent air on four nozzles having circular throats and circular, elliptical, and oval exit cross sections. The plume shapes were photographically recorded from schlieren observations and compared to predictions calculated by the method of reference 2.

SYMBOLS

A_j Exit area, in^2

A_t Throat area, in^2

P_c Chamber pressure, lb/in^2

P_j Exit pressure, lb/in^2

$\dot{m}_A$ mass-flow rate of nozzle A, slug/sec

$\dot{m}_B$ mass-flow rate of nozzle B, slug/sec

$\dot{m}_C$ mass-flow rate of nozzle C, slug/sec

$\dot{m}_D$ mass-flow rate of nozzle D, slug/sec

p_{ma} Measured pressure at orifice located on the exit major axis, lb/in^2

p_{mi} Measured pressure at orifice located on the exit minor axis, lb/in^2

p_∞ Ambient test chamber pressure, lb/in^2

θ Angular orientation of nozzle exit major axis to viewing axis of schlieren system, deg.

APPARATUS AND TESTS

Four nozzles were designed and fabricated for the tests. Sketches of these nozzles illustrating their nominal design dimensions are shown in figure 1 and a photograph of three of the nozzles is presented in figure 2.

All of the nozzles were fabricated from 17-4 stainless steel, and each nozzle had a rounded entrance to a straight-sided circular throat section with an abrupt transition to a conical expansion to the exit plane. The circular throats were selected primarily to facilitate the measurement of their fidelity, thereby insuring that the various nozzle throat dimensions were known. Table 1 lists their characteristics and actual pertinent dimensions as measured subsequent to fabrication. Nozzle A, the baseline nozzle, is an axisymmetric (circular cross-section) nozzle and was used as the basis for comparing the other nozzles. Nozzles B and C were designed with the same throat diameter as nozzle A, but the exit cross sections were an ellipse and a straight-sided oval, respectively, with their major axes equal to the diameter of nozzle A. The resulting exit areas were approximately one-half that of nozzle A, with correspondingly lower expansion ratios and higher exit-to-ambient pressure ratios for a given chamber pressure. Conversely, nozzles B and C would require less than half the chamber pressure and mass flows as nozzle A to produce the same exit-to-ambient pressure ratio. As shown in figure 1, nozzle D has approximately the same exit ellipse as nozzle B, but the throat area was approximately one half that of the other nozzle; thus, the expansion ratio was about equal to that for nozzle A. For a given chamber pressure, nozzle D would be expected to produce the same exit-to-ambient pressure ratio for about half the mass flow as nozzle A. Since the nozzles had circular throat cross sections it is recognized that the transition in cross section at the throat from circular to elliptical or oval would produce uneven expansion of the flow in the nozzle and therefore affect the exit flow characteristics of the asymmetric nozzles B, C, and D.

Each nozzle had 2 pressure orifices near the exit consisting of 0.040 in. o.d., 0.020 in. i.d. stainless steel tubing silver-soldered flush with the nozzle wall and exit-plane surface and hand worked to a smooth surface at the orifice. As the centers of the orifices were located 0.020 in. upstream of the exit plane the pressures at these locations would be somewhat higher than the actual exit pressures as the flow was still expanding. Exit pressures were calculated for these locations for each nozzle for comparison with the actual measurements.

The tests were conducted in the Langley Nozzle Test Chamber. A photograph of the test chamber is shown in figure 3, and a detailed description is given in reference 3. The Nozzle Test Chamber is a sealed chamber connected to a vacuum system capable of evacuating the chamber to pressures as low as one millimeter of mercury. The system contains several large vacuum storage spheres (40 ft., 60 ft., and 100 ft. in. diameter) that in conjunction with the pumps can maintain an essentially quiescent environment at low pressure (which varied slowly with time) while the nozzles are operating. A schematic diagram of the nozzle test chamber and gas supply system is shown in figure 4(a). Dry, unheated high pressure air is supplied to the nozzle test fixture. An adaptor plate (figure 4(b)) designed to hold the nozzles was bolted directly to this test fixture. The test chamber is equipped with opposing windows and a double-pass, parallel light schlieren system having a continuous light source. A movable mirror can be positioned for viewing the image on a video monitor or for single-frame exposure on a film plate.

Each nozzle was tested for a range of plenum pressures, from 32 to 190 psia at ambient pressures ranging from 0.021 to 0.113 psia. The plenum

pressure was limited to 200 psi or less because of structural limitations in the nozzle test fixture. At each test point simultaneous measurements of plenum pressure and temperature, ambient chamber pressure and temperature, nozzle exit pressure, and schlieren photographs of the plumes were recorded. Each non-circular nozzle was tested with the major axis in the exit plane transverse to the line of sight across the test chamber and again with the nozzle rotated 90° about its longitudinal axis. In this way two orthogonal views of the plume profiles were obtained for, in most cases, the same exit-to-ambient pressure ratio, P_j/P_∞. The exit-to-ambient pressure ratios were determined by dividing the calculated nozzle exit pressure by the measured test chamber static pressure. The nozzle exit pressure was determined from reference 4, assuming an isentropic, inviscid expansion from the measured plenum chamber pressure and temperature and the corresponding nozzle physical characteristics given in table I. The orifice pressures near the nozzle exits were calculated in the same manner. The uncertainties in the pressure measurements are unknown, but the differences in the measurements when the test chamber was pumped down prior to a test were obtained. The difference between the measured orifice pressures and the ambient pressure at zero chamber pressure ranged from plus 0.004 to .016 psi, depending upon the gage. One gage consistently indicated 0.012 psi higher than the other and both gages consistently indicated higher pressures than the ambient pressure measurement. This consistent positive difference could be caused by leaks in the nozzle pressure system (the nozzles were changed frequently without leak checks) or lag in the small pressure tubes, or both. Assuming that the deviation of 0.016 psi mentioned above remained during the tests, the errors in the measured

pressures near the nozzle exits would range from 1.2 to 4 percent at the highest and lowest chamber pressure respectively, exclusive of the uncertainties. Additional errors in the pressure measurements during tests with flow through the nozzles could occur because of the relatively small dimensions of these nozzles. Small fabrication errors could result in large errors in the measured pressures compared to the predicted values. The nozzle throat and exit dimensions were determined with an uncertainty of 0.0005 in., but imperfections in the nozzle expansion regions could not be determined.

PRESENTATION OF DATA

The basic data consisting of schlieren photographs of the exit plane of various exit-to-ambient pressure ratios are presented in figures 5 to 8. For the asymmetric nozzles (figures 6 to 8), the photographs for exit pressure ratios that were nearly matched were placed together to facilitate direct comparison of the effect of nozzle orientation (major axis parallel or perpendicular to the line of sight). Also presented in figures 6 to 8 are the nozzle A plume shapes at equivalent exit pressure ratios for comparison. Figures 5, 6(c), and 8(c) also presented outlines of the plume shapes calculated for the same conditions by the method of reference 2. This code solves the Euler equations for the computation of inviscid 2-D and axisymmetric underexpanded plumes. Since the calculations were limited to axisymmetric plume shapes, the asymmetric plume data (figures 6(c) and 8(c)) are compared with calculated axisymmetric plumes having the same

exit-to-ambient pressure ratios. The plume shapes of nozzles B, C, and D at exit pressure ratios of 13 to 14 are compared in figure 9 with the exit plume shape of nozzle A at an exit pressure ratio of 6.297.

The variation of measured near-exit pressures, P_{ma} and P_{mi}, with chamber pressure for nozzles A and B are presented in figure 10, and for nozzles C and D in figure 11. The calculated values of these pressures using a one-dimensional isentropic expansion for the same exit-to-throat area ratios are also presented for comparison. As shown in figure 10, the measured pressures for the two orifices on nozzle A do not agree; one value is about 30 percent higher than the other measurement and the calculated value. A later test conducted after the conical nozzle interior was reworked and polished, hence resulting in minor changes to the contour, showed better agreement between the two measurements although both measurements were markedly different than the original ones. This indicates that the nozzle characteristics are very sensitive to manufacturing imperfections. The measured pressures of nozzle A and nozzle D are compared (they have nearly the same expansion ratio) with the calculated values in figure 12. The pressures measured on the major axis of nozzle D and one set measured for nozzle A agree closely with the calculated values.

RESULTS AND DISCUSSION

As stated previously, the primary objective of the tests was to compare the circular nozzle plume shapes to the non-circular nozzle plume shapes at the same exit pressure ratios. From these comparisons, the effectiveness of reducing the nozzle exit area by reducing the nozzle exit

dimension in one direction only can be evaluated. Because of the upper limit on plenum pressure, the maximum exit-to-ambient pressure ratio obtainable for nozzle A was somewhat lower than those obtained with nozzles B and C. The plume shapes for nozzles B and C for exit pressure ratios higher than the maximum obtained with nozzle A were therefore compared to the calculated plume shapes. Figure 5 shows that the calculated plume shapes for nozzle A closely resemble the actual shapes taken from the schlieren photographs. This provides assurance that the calculated plumes would provide a measure for assessing the plumes of the asymmetric nozzles for cases where there are no corresponding data for the axisymmetric nozzle A.

In general, at the lower exit-to-ambient pressure ratios, the asymmetric nozzles B, C, and D produced smaller plume widths in the major and minor axes than the plumes of nozzle A at comparable exit pressure ratios [figures 6(a), 7(a), 7(b), 8(a), and 8(b)]. In this range of exit pressure ratios (6.0 to 14.0 for nozzles B, C, and D) the pressure ratio was not a reliable indicator of the plume width for the asymmetric nozzles. In all of these cases, the exit pressure ratios, and correspondingly the chamber pressures and mass flows, would have to be increased to match the corresponding plume of nozzle A. For example, it can be noted that the plumes produced by nozzles B, C, and D at exit pressure ratios of 13 to 14 more closely match the exit plume shape of nozzle A at an exit pressure ratio of 6.297 (see figure 9). The calculated ratios of the mass flows of nozzles B, C, and D at exit pressure ratios of approximately 12 to 14 to the mass flow of nozzle A at an exit pressure ratio of 6.297 are also shown in figure 9.

The plume shapes produced by nozzles B, C, and D, at exit pressure ratios of approximately 30 or greater compared favorably with those of nozzle A [figures 6(b), 7(c), and 8(d)] or the calculated shapes [figures 6(c), 7(d), and 8(c)] at the same exit pressure ratios. In all of these cases, the width of the plumes emanating in the plane of the nozzle minor axes (θ=0°) of the non-circular nozzles was larger than those in the plane of the major axes (θ=90°). This might be expected because of the uneven expansion within the nozzle resulting from the transition from the circular throat to the final oval or elliptical cross-sectional shape at the nozzle exit plane. This is borne out by the measured pressures near the exits for nozzles B, C, and D (figures 10, 11, and 12 respectively) being higher on the minor axes than those measured on the major axes. Although the flow within the nozzles was probably highly 3-dimensional, the measured pressures indicate that the flow inside the nozzles expanded less in the plane of the minor axis. The dashed lines in these figures represent the calculated pressures at the orifice location for circular nozzles having the same expansion ratios as the test nozzles.

Referring back to figures 6(b) and 6(c) it can be seen that for exit pressures nearly the same [figure 6(b)], the plume widths of nozzle B (exit pressure ratios of 60-61) are only slightly smaller than that for nozzle A at an exit pressure ratio of 59.14. The nozzle B plumes, when increased to exit pressure ratios of 68-71 compare more closely with the nozzle A plume at the lower exit pressure ratio [figure 6(c)]. The calculated mass flows of nozzle B at exit pressure ratios of 60-61, and 68-71 [figures 6(b) and

6(c)], when adjusted to the ambient conditions of nozzle A, range from about 36 percent to 42 percent respectively, of that of nozzle A at an exit pressure of 59.14.

The calculated mass flows for nozzle C for the cases where the plumes at the higher exit pressure ratios compared favorably with that of nozzle A (figure 7(c)) averaged about 43 percent of that of nozzle A at the same exit pressure ratio. The same trend is noted for nozzle D; where the exit pressure ratios are nearly the same as that for nozzle A (figure 8(d)), the calculated mass flows are about 55 percent of that of nozzle A. The preceding discussion has shown that at low exit-to-ambient pressure ratios (approximately 15 or less), the non-circular nozzles B, C, and D produced smaller plumes than those produced by the circular nozzle A for the same exit conditions. Higher exit pressure ratios and, consequently, higher mass flows would be required to establish plume shapes comparable to that produced by a circular nozzle. This would tend to negate any advantage in designing model test nozzles with reduced exit areas and non-circular exit shapes. On the other hand, the reverse was true at exit-to-ambient pressure ratios of 30 and above. At comparable exit pressure ratios, the plume shapes of the non-circular nozzles compared favorably with those produced by the circular nozzle and the mass flows were reduced to values near those predicted for the same exit-to-ambient pressure ratios. The nozzles having the lower expansion ratios (nozzles B and C) required lower mass flows than the nozzle with the same expansion ratio (nozzle D) as the circular nozzle A.

CONCLUDING REMARKS

Tests were conducted on a series of model nozzles in the Langley Nozzle Test Chamber to determine the qualitative effects of nozzle expansion ratio and exit cross-sectional shape on the exit plume shape and mass flows. The results of the tests conducted on a series of model nozzles having circular throats with circular, elliptic, and oval exit cross sections exhausting dry, unheated air into quiescent air indicated that, at exit-to-ambient pressure ratios of 30 and above, exit plumes equivalent in size and shape to circular nozzle plumes could be generated by the non-circular nozzles with lower chamber pressures and mass flow rates. This was not true for cases at exit pressure ratios below 15. The exit pressure ratios of the non-circular nozzles in these cases would have to be considerably larger than that of the circular nozzle in order to generate comparable exit plumes. At these lower exit pressure ratios, the resulting mass flows for the non-circular nozzles having lower expansion ratios were only slightly less than that of the circular nozzle and somewhat higher than the circular nozzle for the non-circular nozzle having the same expansion ratio.

REFERENCES

1. Pindzola, M.: Jet Simulation in Ground Test Facilities. AGARDograph 79, November 1963.

2. Salas, Manuel D.: The Numerical Calculation of Inviscid Plume Flow Fields. AIAA Paper 74-523, June 1974.

3. Keyes, J. Wayne: Modifications to the Nozzle Test Chamber to Extend Nozzle Static - Test Capability. NASA TM 86368, May 1985.

4. Ames Research Staff: Equations, Tables and Charts for Compressible Flow. NACA TR1135, 1953.

TABLE I. - NOZZLE CHARACTERISTICS

Nozzle A - Circular Exit	
Throat diameter, in.	0.0815
Exit diameter, in.	0.252
Throat area, A_t, sq. in.	0.0052168
Exit area, A_j, sq. in.	0.049876
Area ratio, exit-to-throat, A_j/A_t	9.561
Exit Mach number	3.872
Pressure ratio, P_j/P_c	0.00782
Nozzle B - Elliptical Exit	
Throat diameter, in.	0.081
Exit major axis, in.	0.250
Exit minor axis, in.	0.1275
Throat area, A_t, sq. in.	0.0051529
Exit area, A_j, sq. in.	0.025034
Area ratio, exit to throat, A_j/A_t	4.85824
Exit Mach number	3.145
Pressure ratio, P_j/P_c	0.02193
$\dot{m}_B/\dot{m}_A$ at equal exit pressure*	0.3521
Nozzle C - Oval Exit	
Throat diameter, in.	0.081
Exit major axis, in.	0.2526
Exit minor axis, in.	0.1173
Throat area, A_t, sq. in.	0.0051529
Exit area, A_j, sq. in.	0.026677
Area ratio, exit to throat, A_j/A_t	5.17712
Exit Mach number	3.21
Pressure ratio, P_j/P_c	0.02039
$\dot{m}_C/\dot{m}_A$ at equal exit pressure*	0.3881
Nozzle D - Ellptical Exit	
Throat diameter, in.	0.060
Exit major axis, in.	0.250
Exit minor axis, in.	0.1377
Throat Area, A_t, sq. in.	0.002827
Exit area, A_j, sq. in.	0.027037
Area ratio, exit to throat, A_j/A_t	9.565973
Exit Mach number	3.873
Pressure ratio, P_j/P_c	0.00782
$\dot{m}_D/\dot{m}_A$ at equal exit pressure*	0.5424

Note: Linear dimensions are measured values.

*At equal exit pressures, $\dot{m}_1/\dot{m}_2 = (P_{c1}/P_{c2})(A_{t1}/A_{t2})$

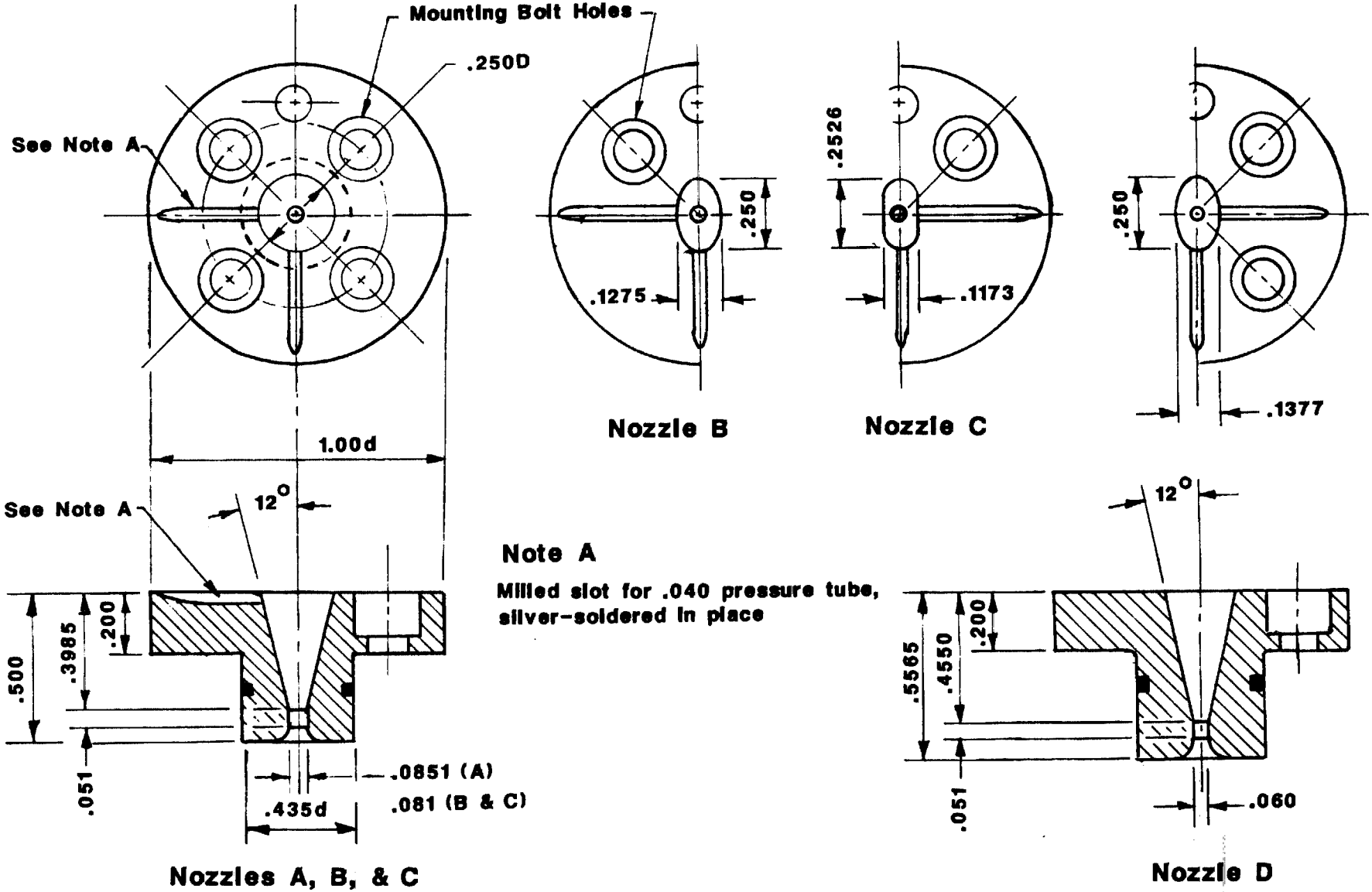

Figure 1.- Sketches of the test nozzles.

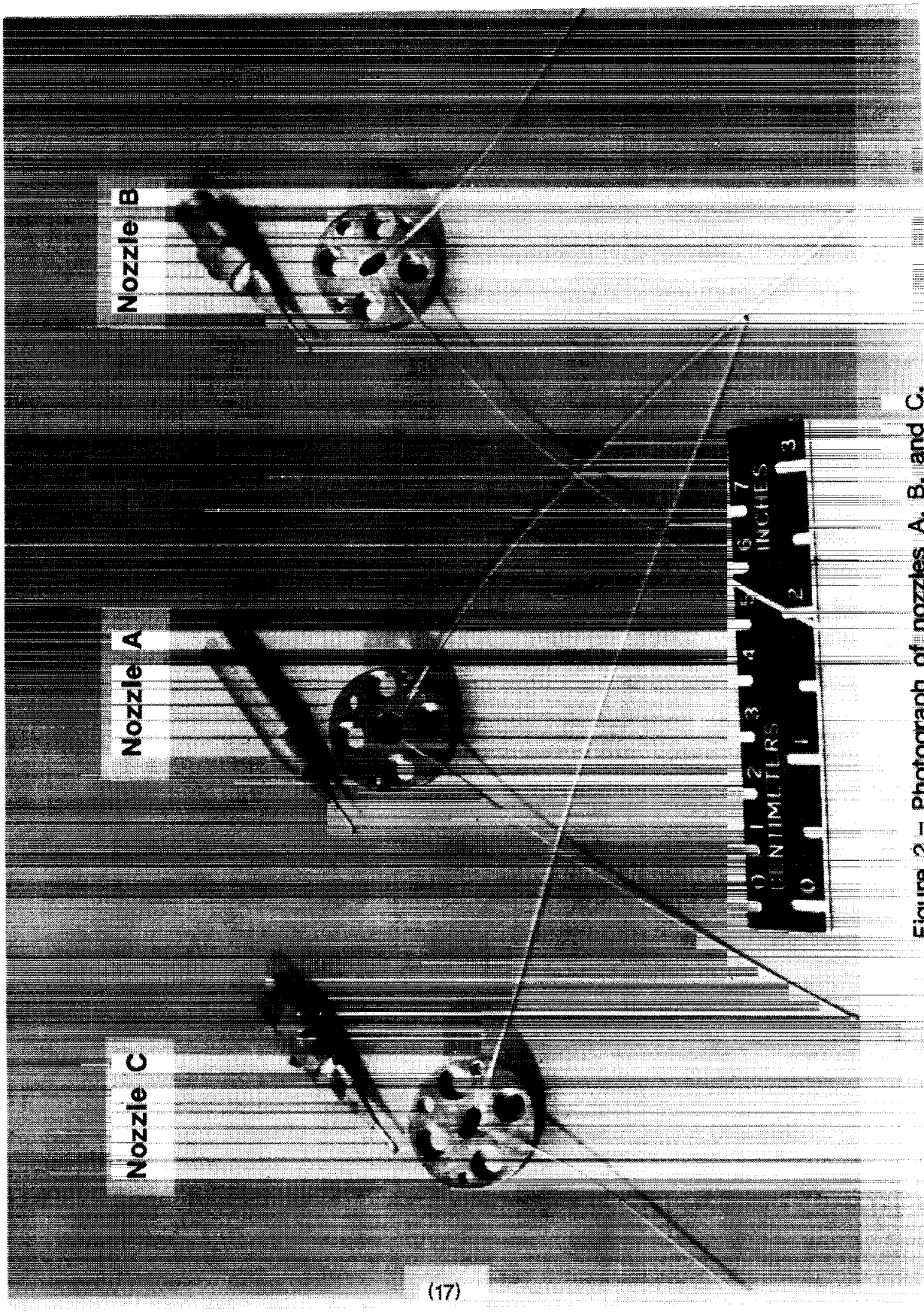

Figure 2.– Photograph of nozzles A, B, and C.

ORIGINAL PAGE
BLACK AND WHITE PHOTOGRAPH

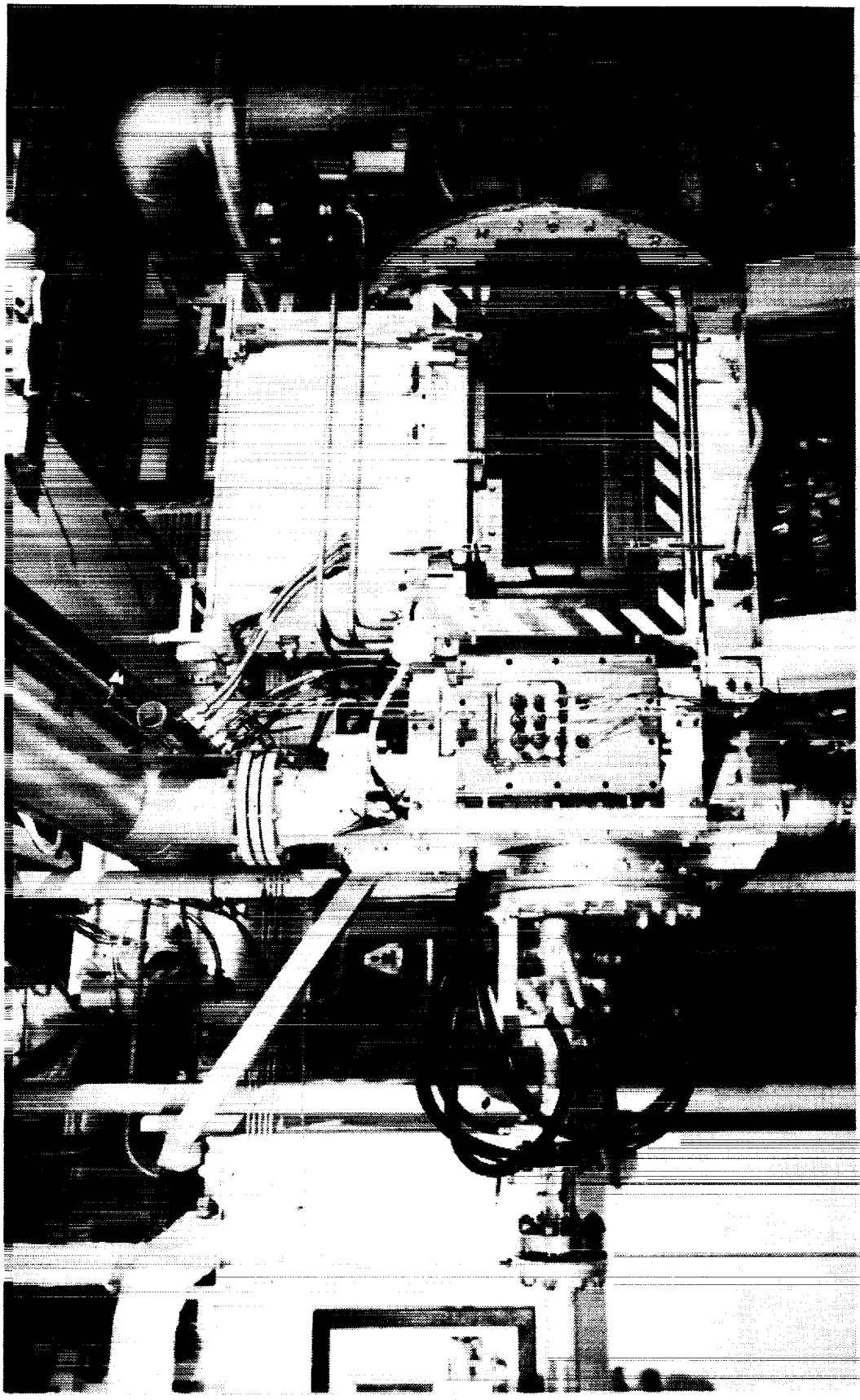

Figure 3.- Photograph of the Nozzle Test Chamber.

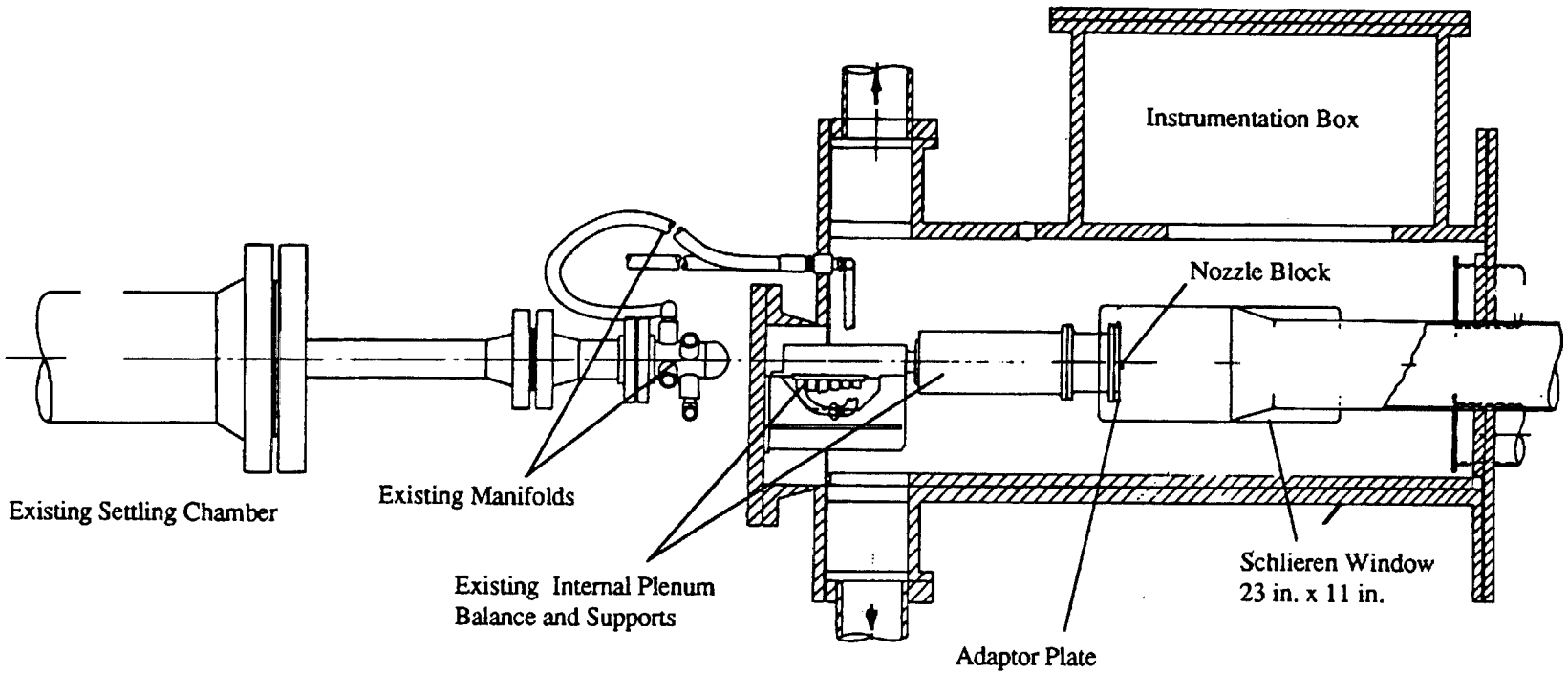

(a) Complete test setup

Figure 4.– Equipment and installation in the Nozzle Test Chamber.

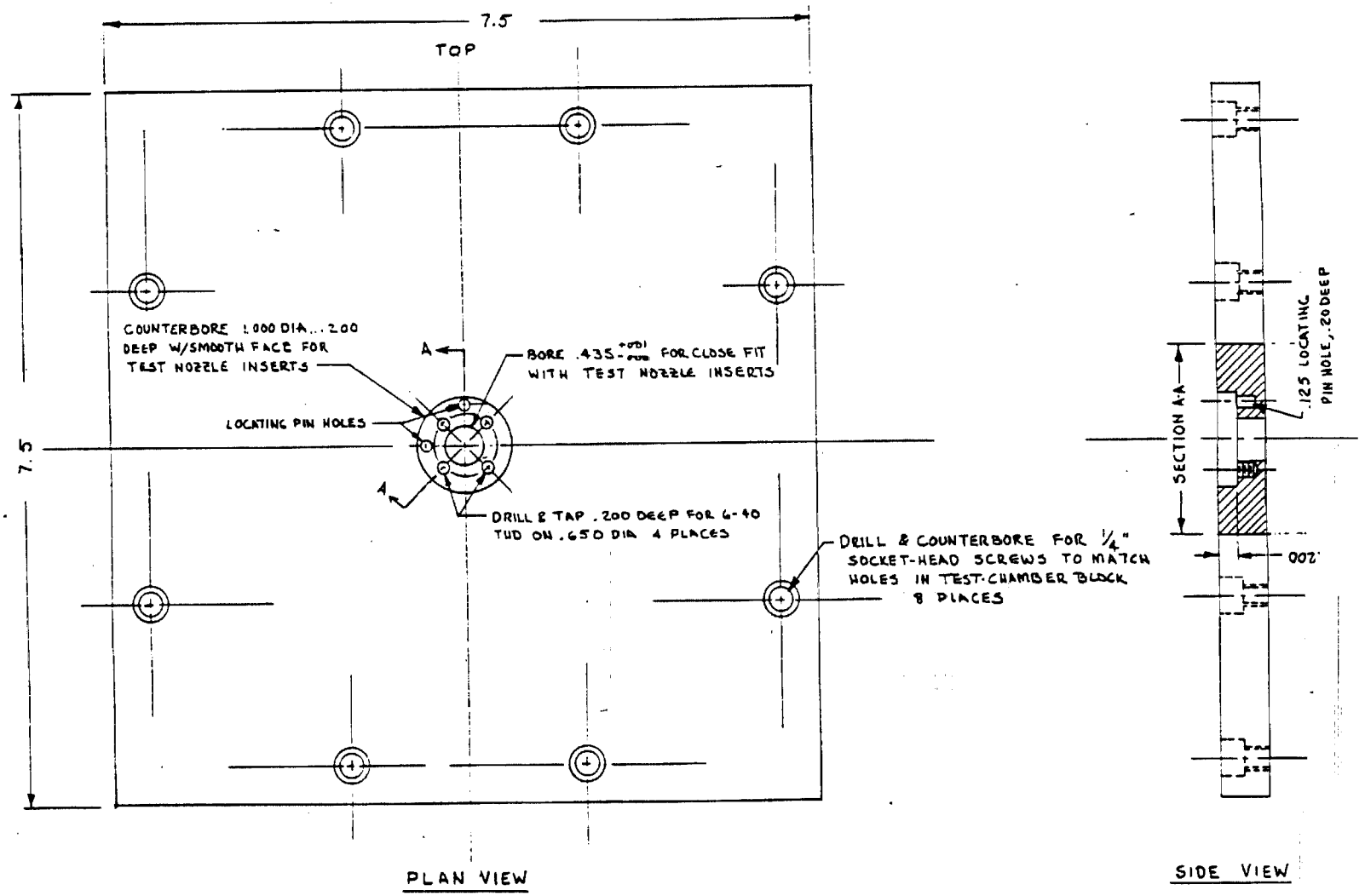

(b) Nozzle adaptor plate

Figure 4.– Concluded.

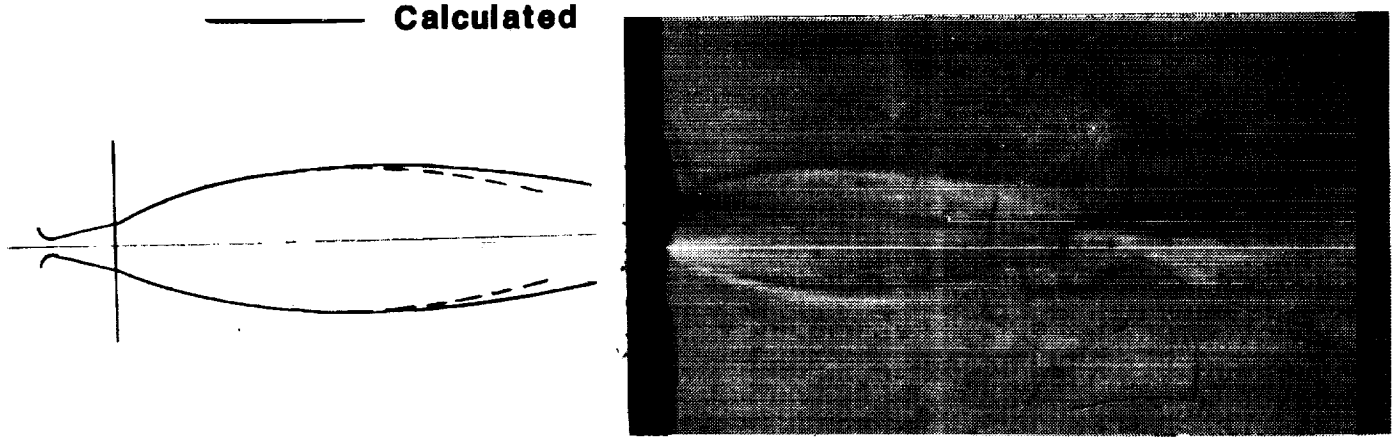

(a) P_j/P_∞ = 6.297; Pc = 90.4, P_∞ = 0.111.

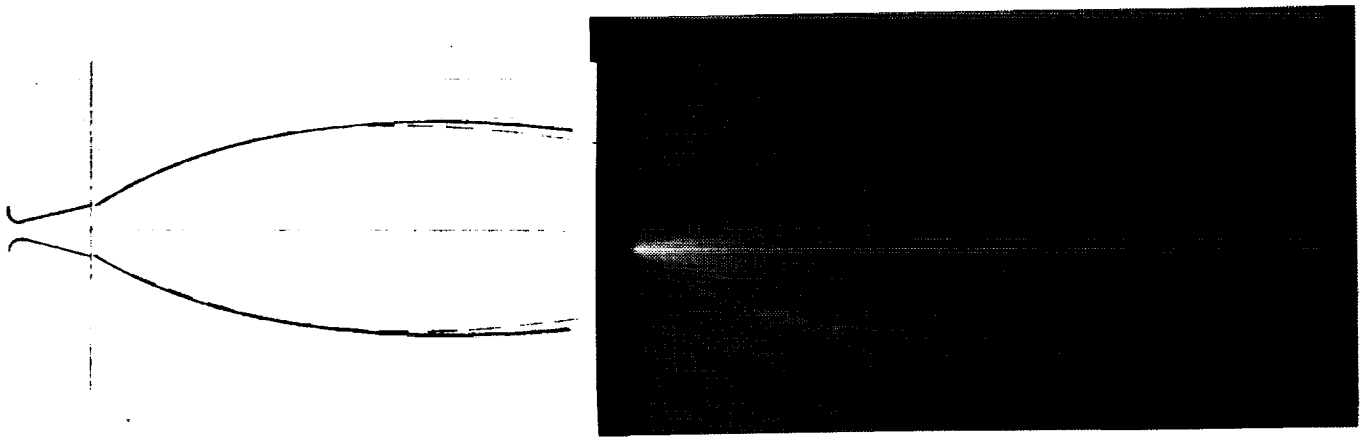

(b) P_j/P_∞ = 13.596; Pc = 150.2, P_∞ = 0.0855.

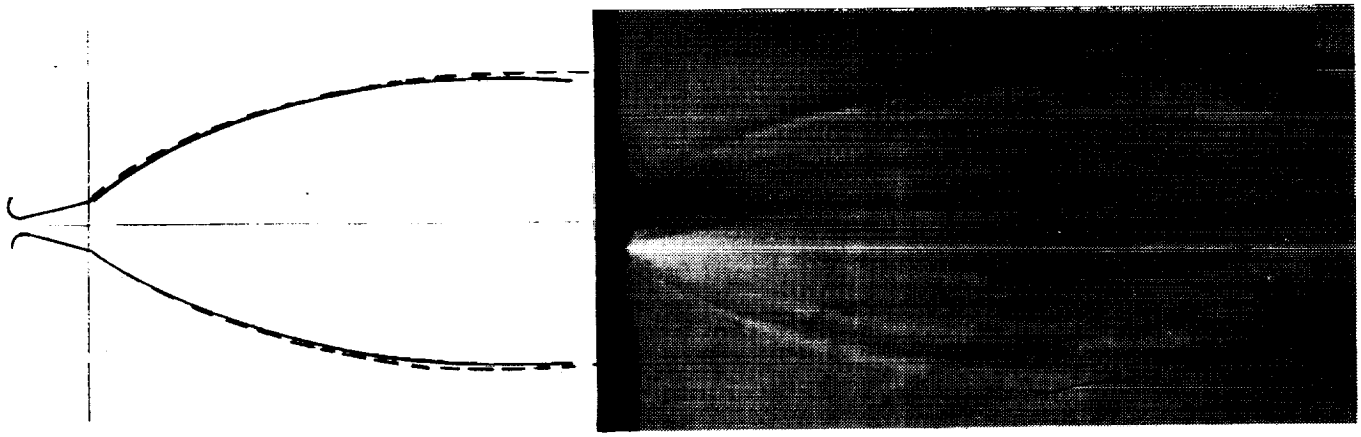

(c) P_j/P_∞ = 29.534; Pc = 190.8, P_∞ = 0.054.

Figure 5.– Comparison of plume shapes as obtained from schlieren photographs and as calculated for nozzle A .

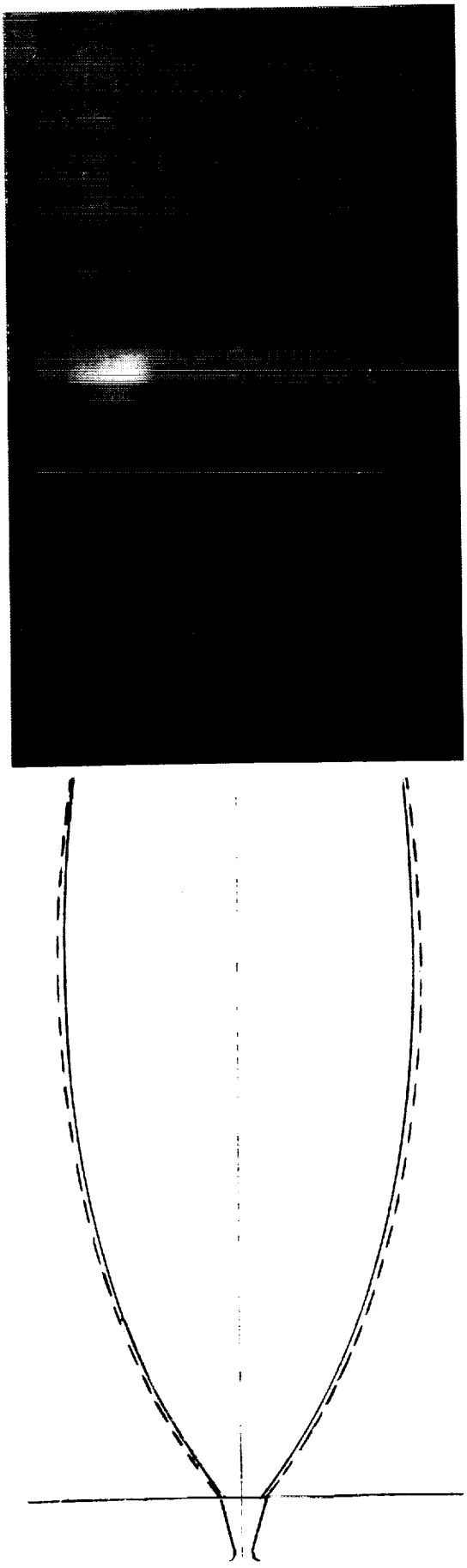

- - - - From Photograph

——— Calculated

(d) P_J/P_∞ = 59.14; Pc = 180.0, P_∞ = 0.0238.

Figure 5.- Concluded.

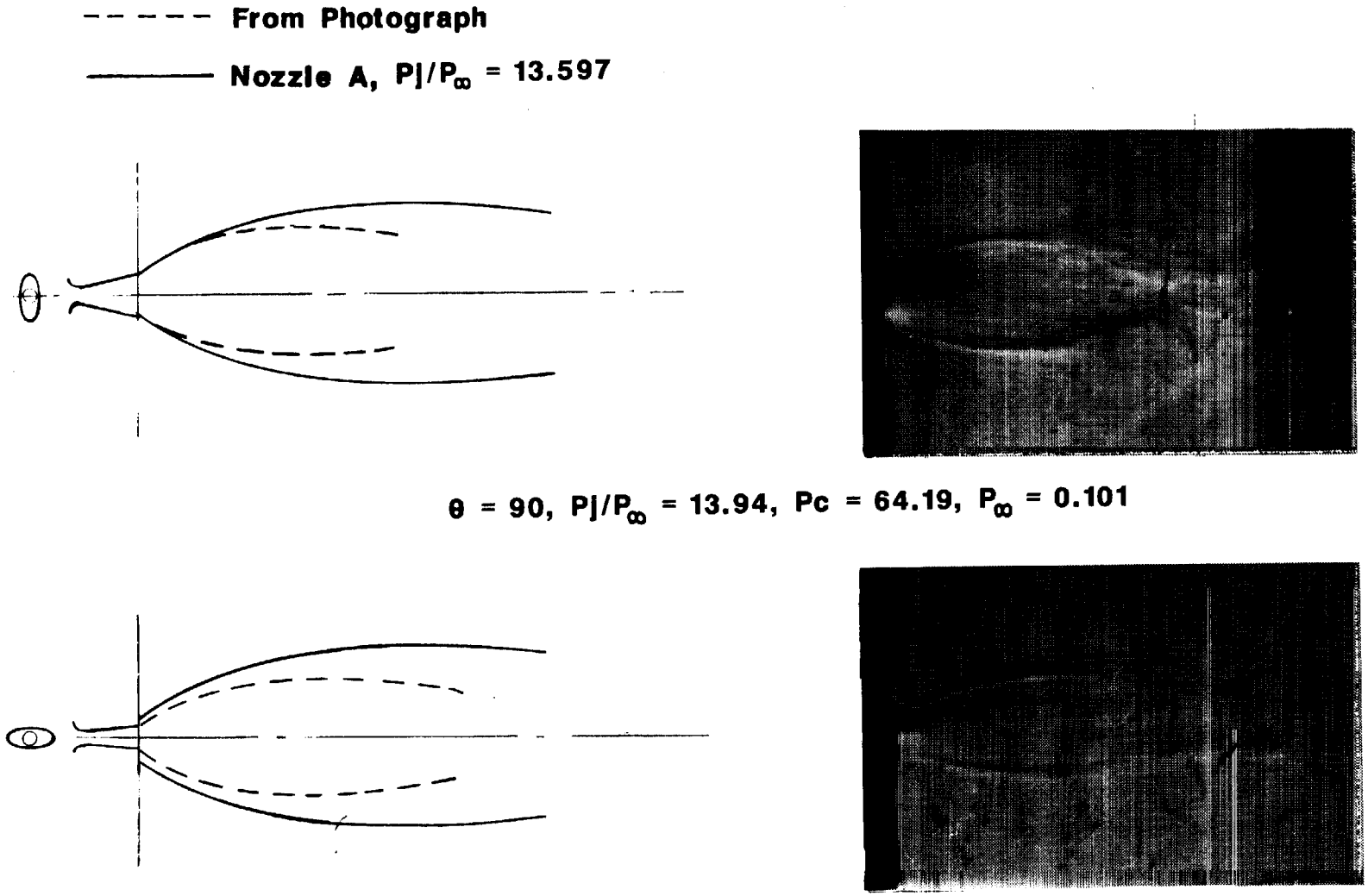

(a) Exit pressure ratios of 13.12 to 13.94.

Figure 6.- Schlieren photographs of the plume shapes produced by nozzle B compared with plume shapes of nozzle A.

– – – – From Photograph
——— Nozzle A, Pj/P_∞ = 59.14

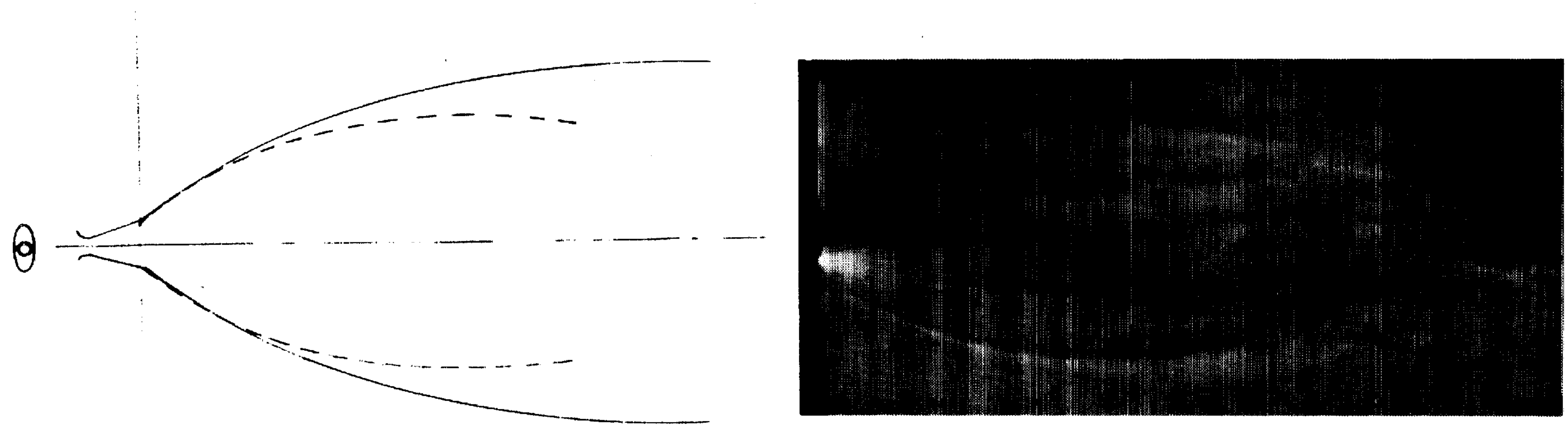

θ = 90, Pj/P_∞ = 61.68, Pc = 135.0, P_∞ = 0.048, m_B/m_A = 0.367

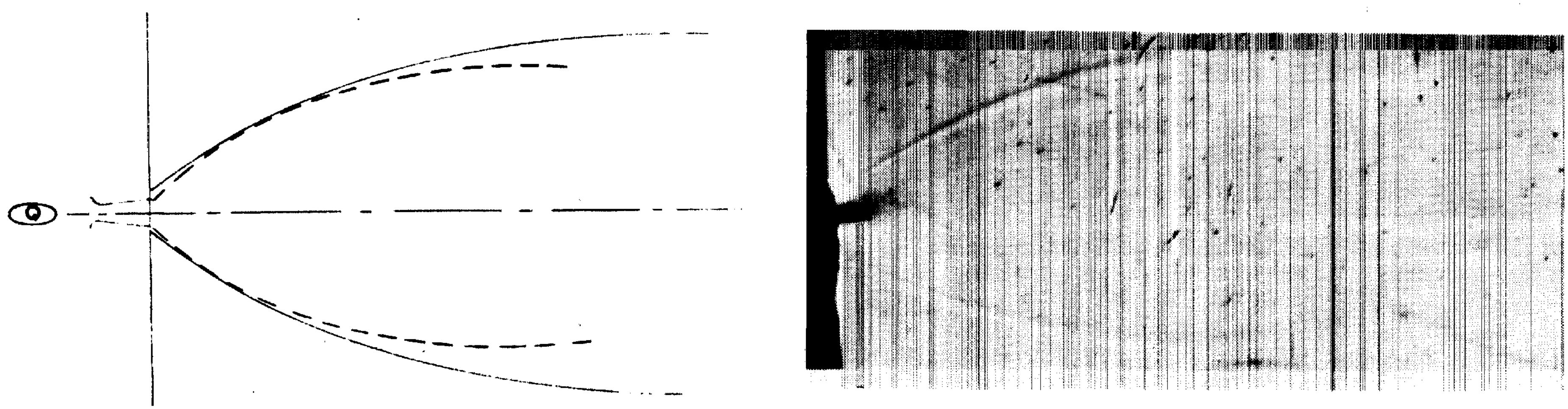

θ = 0, Pj/P_∞ = 60.36, Pc = 115.6, P_∞ = 0.042, m_B/m_A = 0.359

(b) Exit pressure ratios of 60.36 to 61.68.

Figure 6.– Continued.

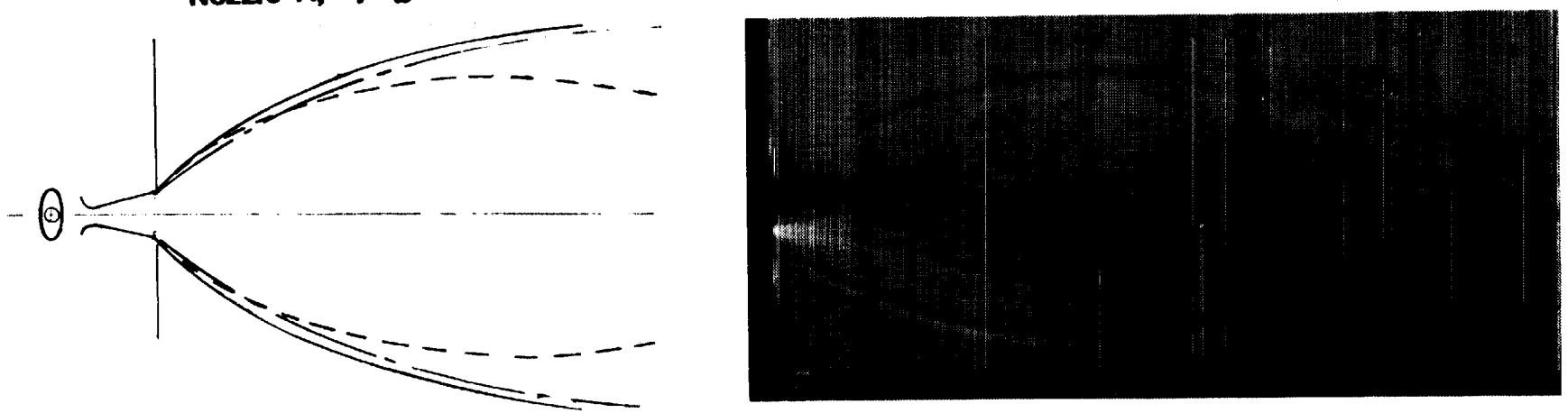

θ = 90, Pj/P∞ = 68.45, Pc = 134.22, P∞ = 0.043, m_B/m_A = 0.408

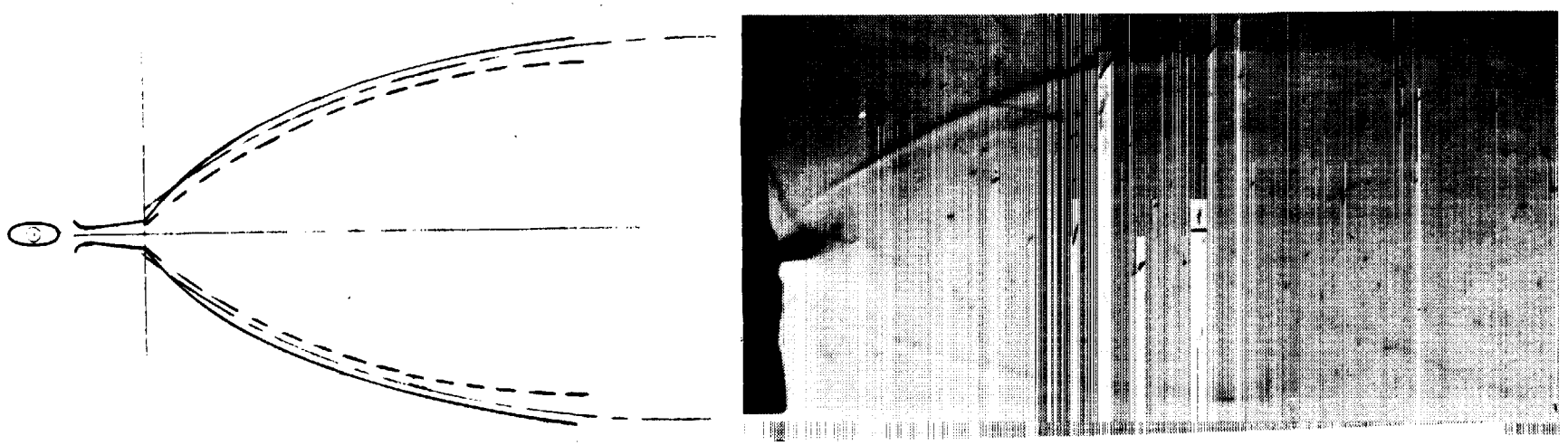

θ = 0, Pj/P∞ = 71.21, Pc = 110.41, P∞ = 0.034, m_B/m_A = 0.424

(c) Exit pressure ratios of 68.45 to 71.21.

Figure 6.– Concluded

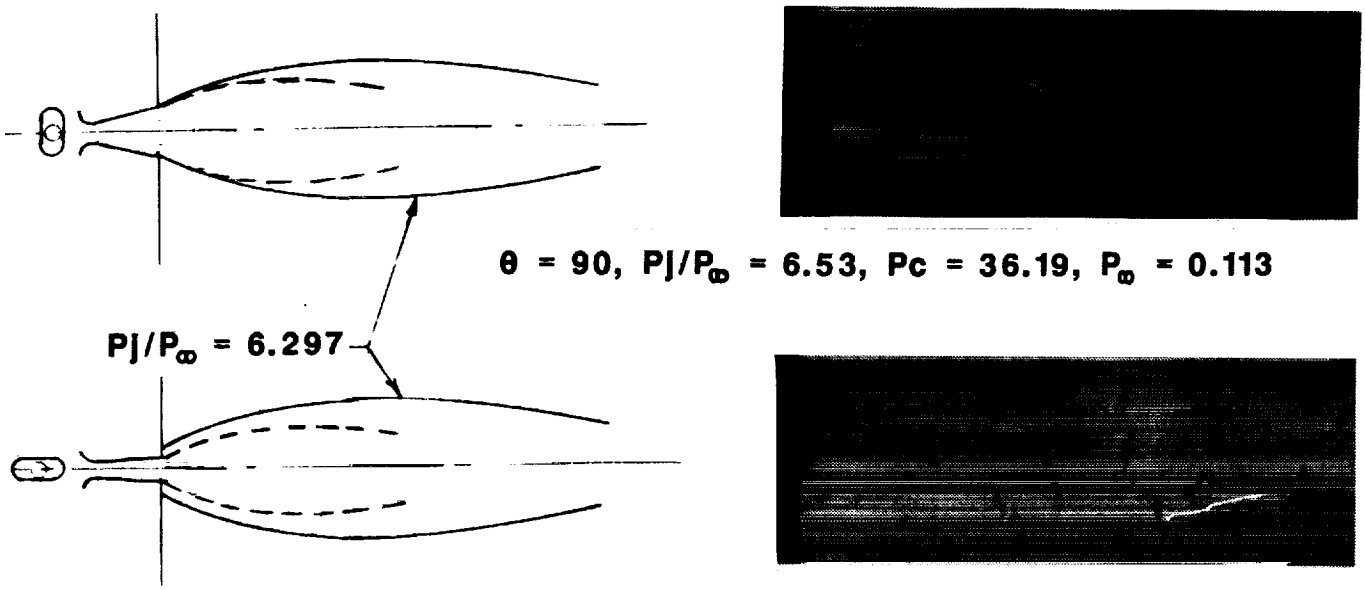

(a) Exit pressure ratios of 6.53 to 6.60.

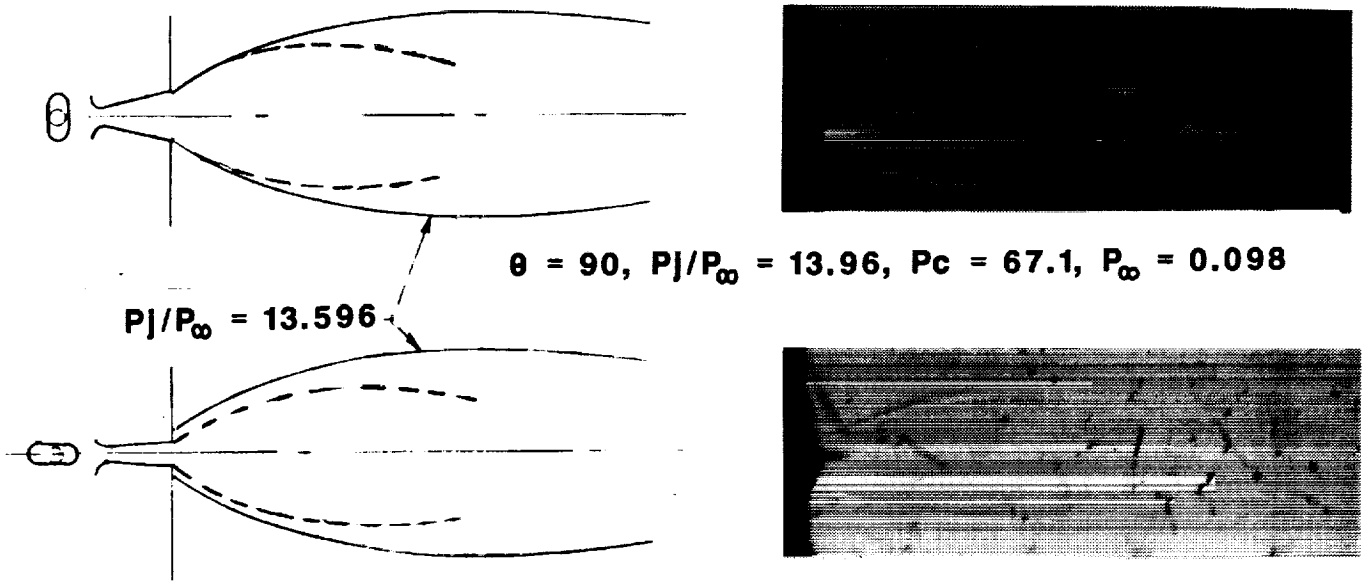

(b) Exit pressure ratios of 13.47 to 13.96.

Figure 7.- Schlieren photographs of the plume shapes produced by nozzle C compared with plume shapes of nozzle A.

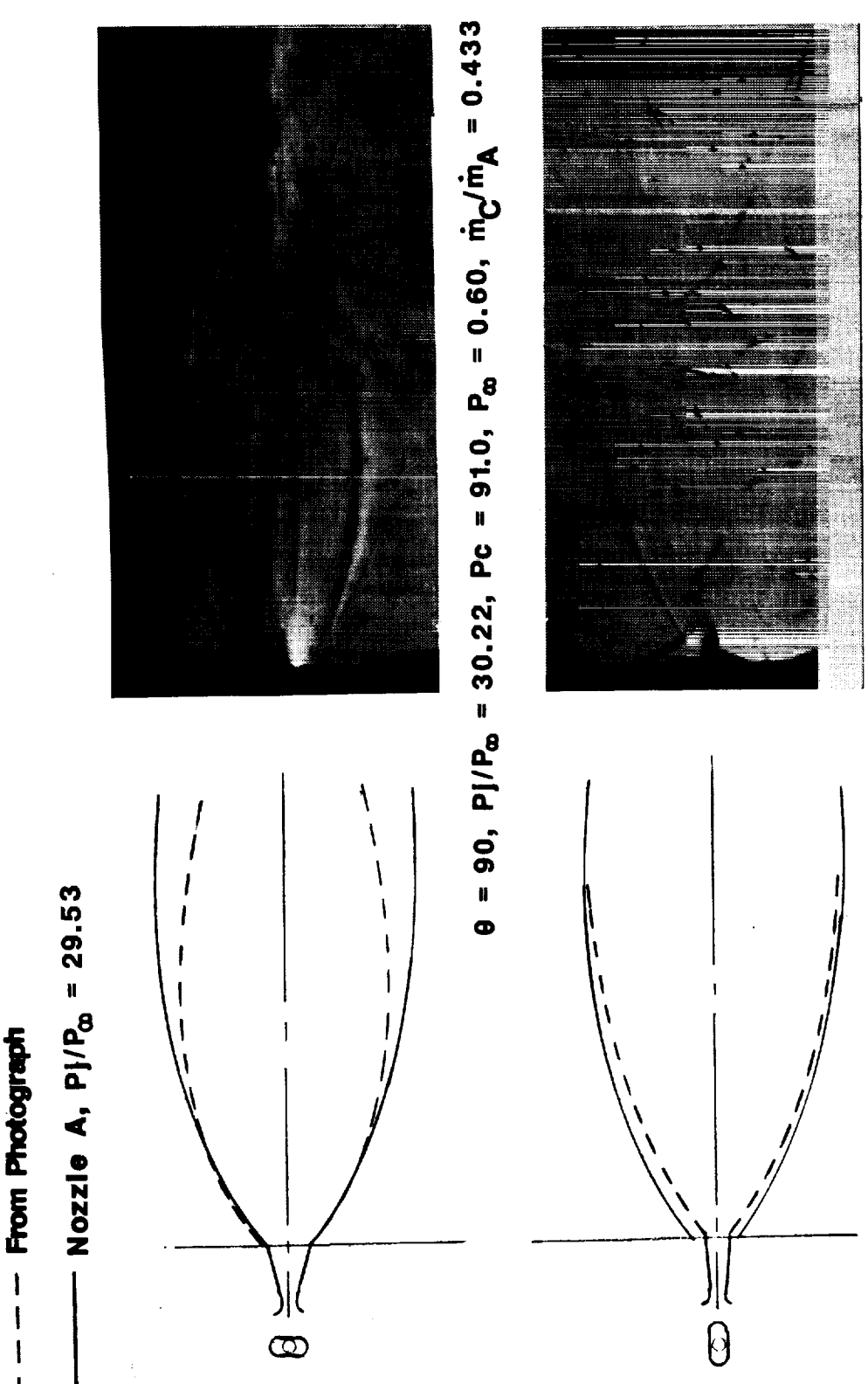

(c) Exit pressure ratios of 30.07 to 30.22.

Figure 7.- Continued.

θ = 90, P_J/P_∞ = 70.99, Pc = 131.81, P_∞ = 0.037

θ = 0, P_J/P_∞ = 72.13, Pc = 126.68, P_∞ = 0.035

(d) Exit pressure ratios of 70.99 to 72.13 .

Figure 7.- Concluded.

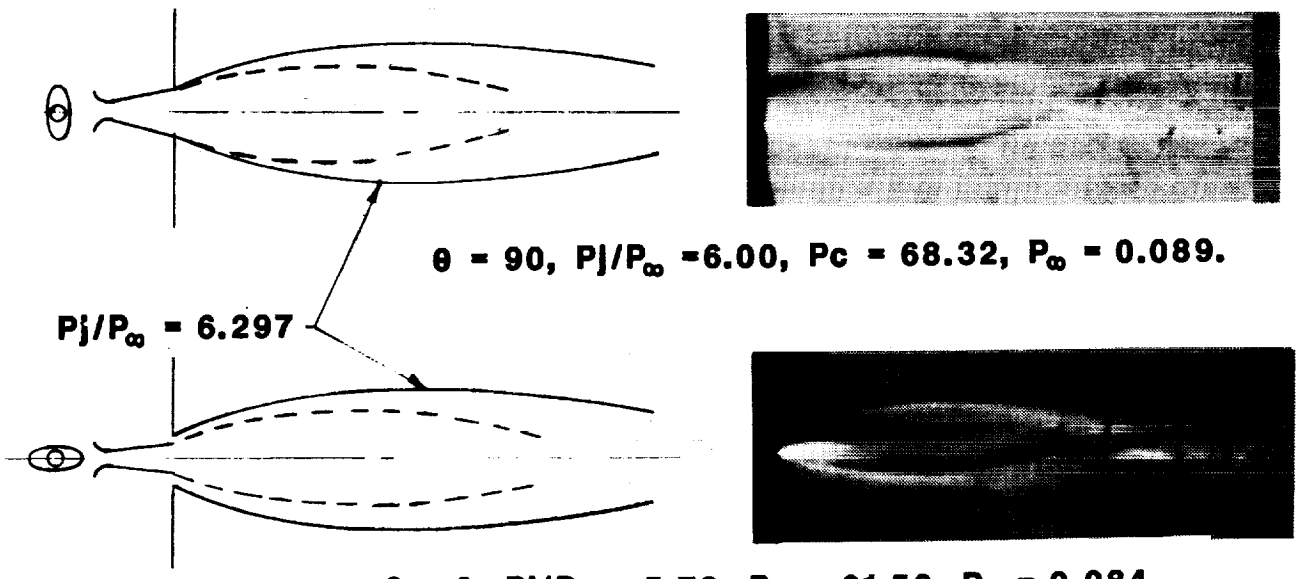

(a) Exit pressure ratios of 5.73 to 6.00.

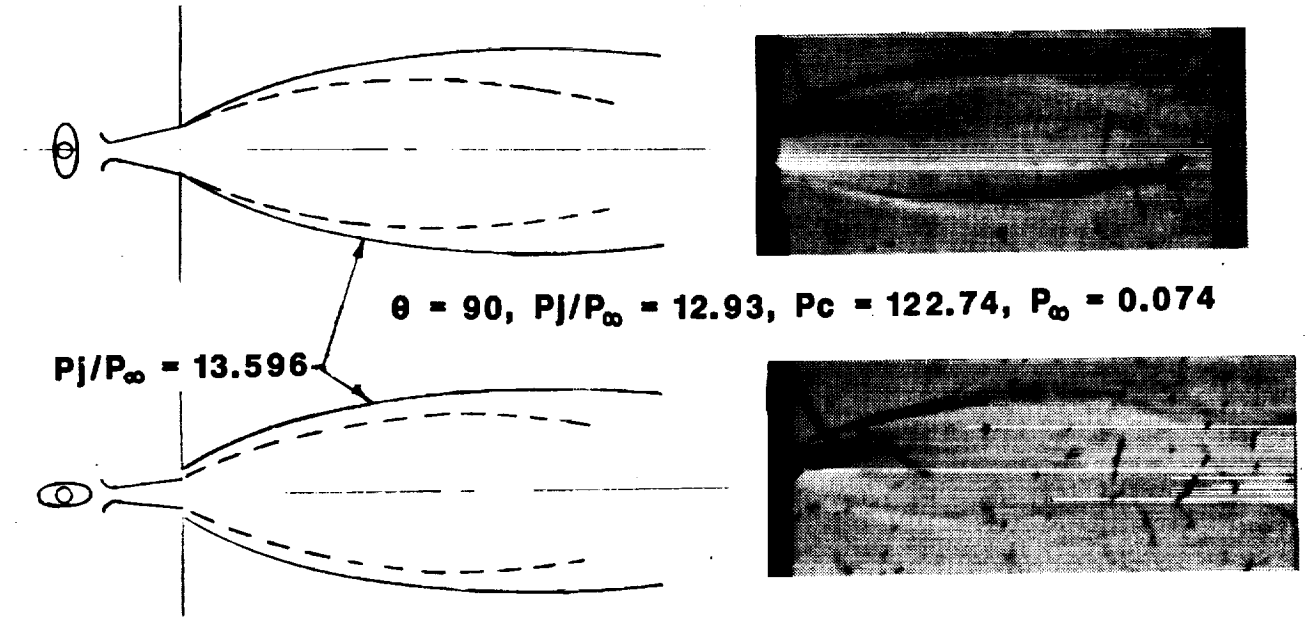

(b) Exit pressure ratios of 12.54 to 12.93.

Figure 8.- Schlieren photographs of the plume shapes produced by nozzle D compared with plume shapes of nozzle A.

θ = 90, P_j/P_∞ = 36.23, Pc = 189.96, P_∞ = 0.041

θ = 0, P_j/P_∞ = 35.72, Pc = 191.86, P_∞ = 0.042

(c) Exit pressure ratios of 35.72 to 36.23.

Figure 8.- Continued.

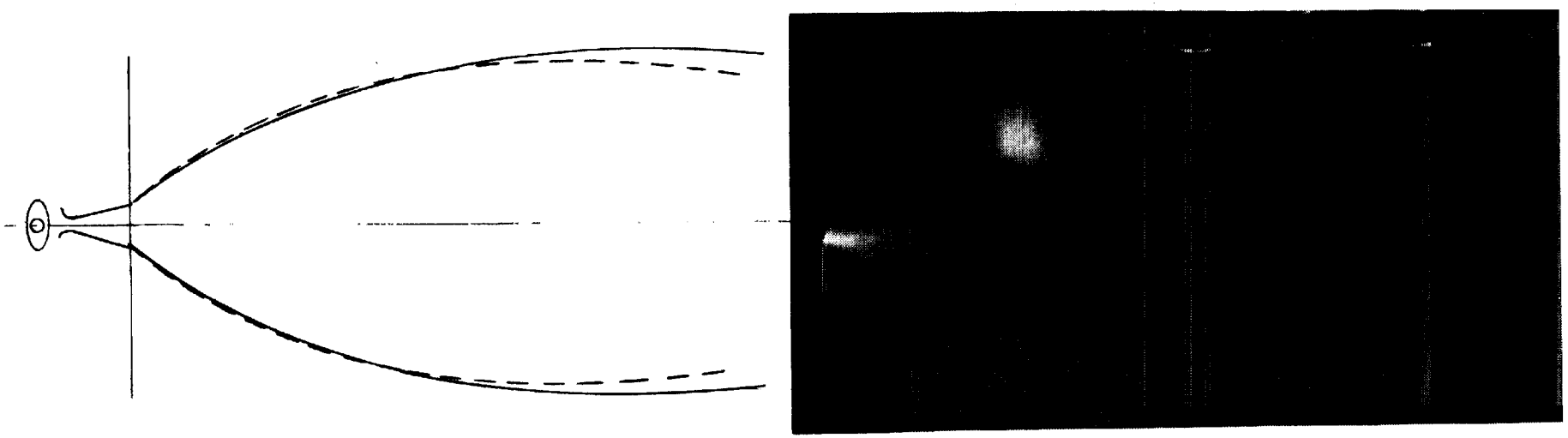

θ = 90, P_j/P_∞ = 60.82, Pc = 178.89, P_∞ = 0.023, $\dot{m}_D/\dot{m}_A$ = 0.546

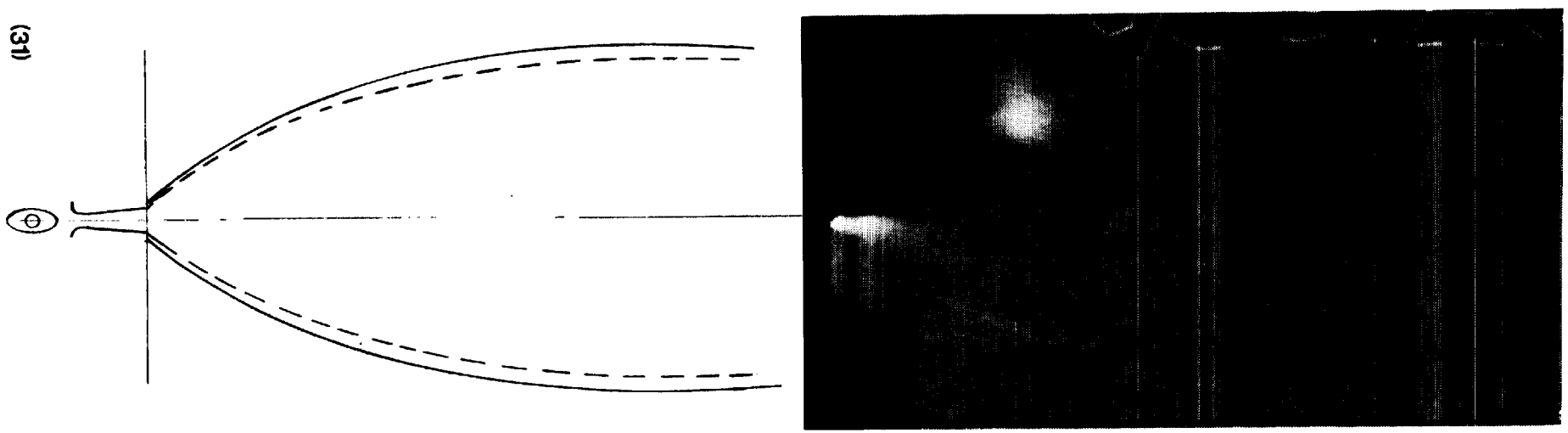

θ = 0, P_j/P_∞ = 58.34, Pc = 179.07, P_∞ = 0.024, $\dot{m}_D/\dot{m}_A$ = 0.535

(d) Exit pressures of 58.34 to 60.82.

Figure 8.- Concluded.

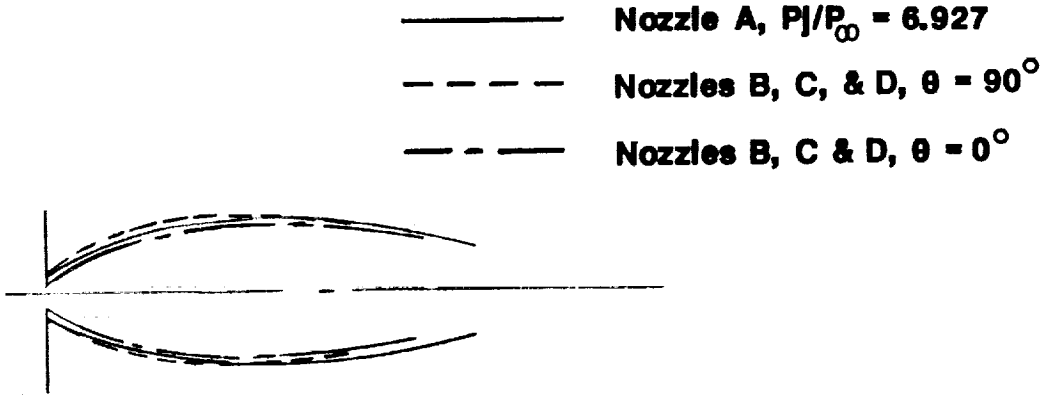

(a) Nozzle B, P_j/P_∞ = 13.12 – 13.94, $\dot{m}_B/\dot{m}_A$ = 0.75 .

(b) Nozzle C, P_j/P_∞ = 13.47 – 13.96, $\dot{m}_C/\dot{m}_A$ = 0.82 .

(c) Nozzle D, P_j/P_∞ = 12.54 – 12.93, $\dot{m}_B/\dot{m}_A$ = 1.08.

Figure 9.– Comparison of the plumes from nozzles B, C, and D at exit pressure ratios ranging from 12.54 to 13.96 with the plume from nozzle A at an exit pressure ratio of 6.927.

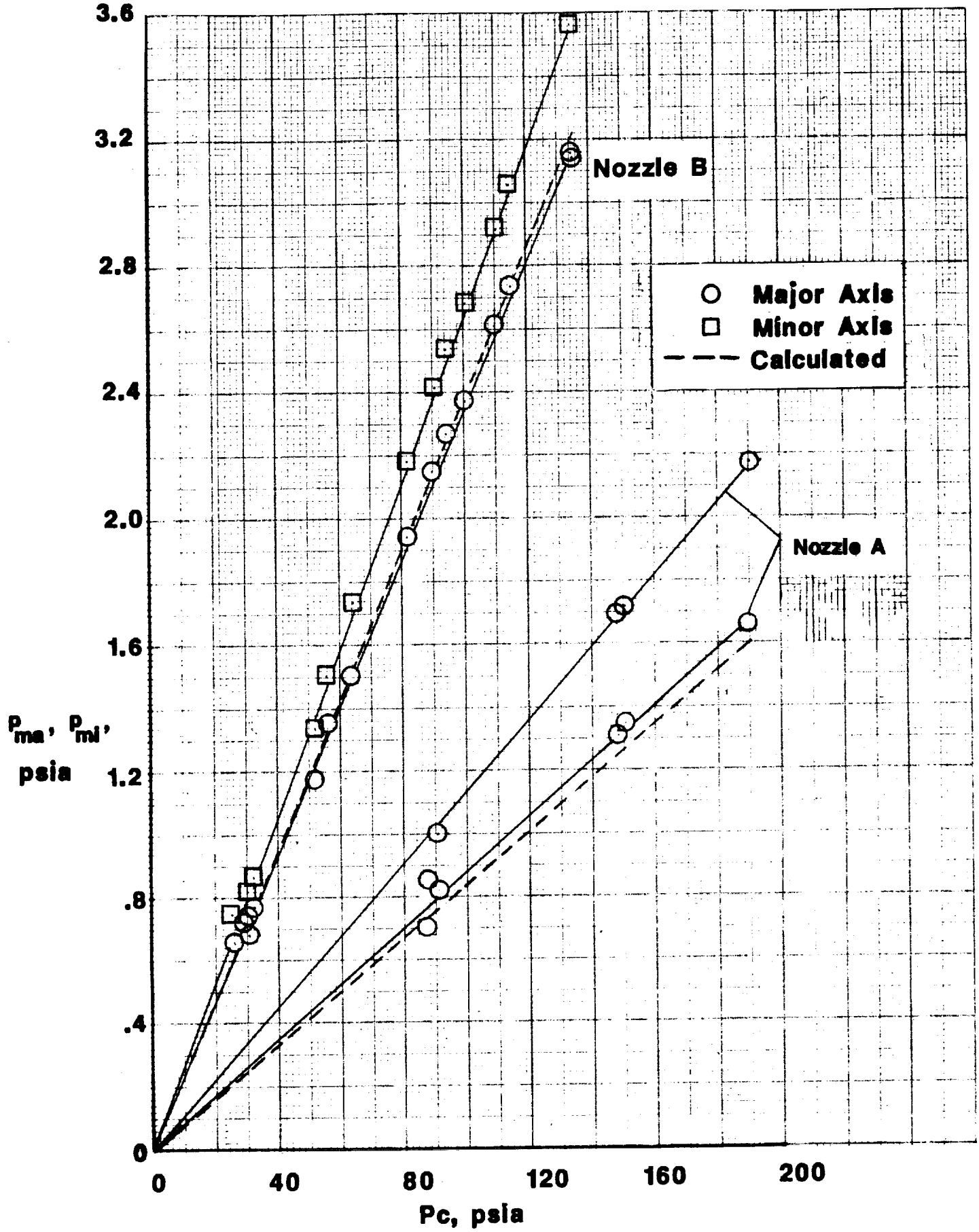

Figure 10.– Variation of pressure near the exit with chamber pressure for nozzles A and B.

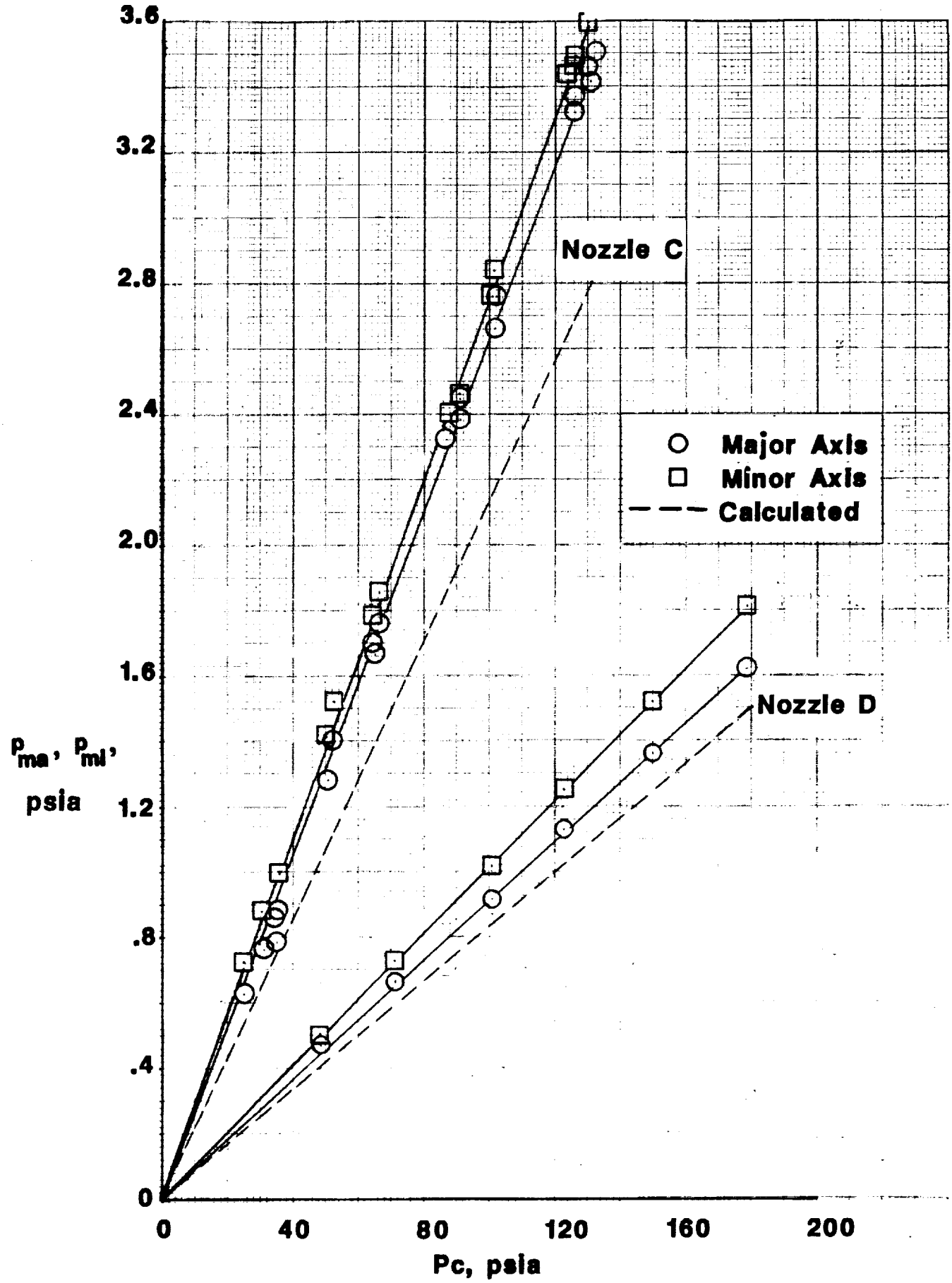

Figure 11.- Variation of pressure near the exit with chamber pressure for nozzles C and D.

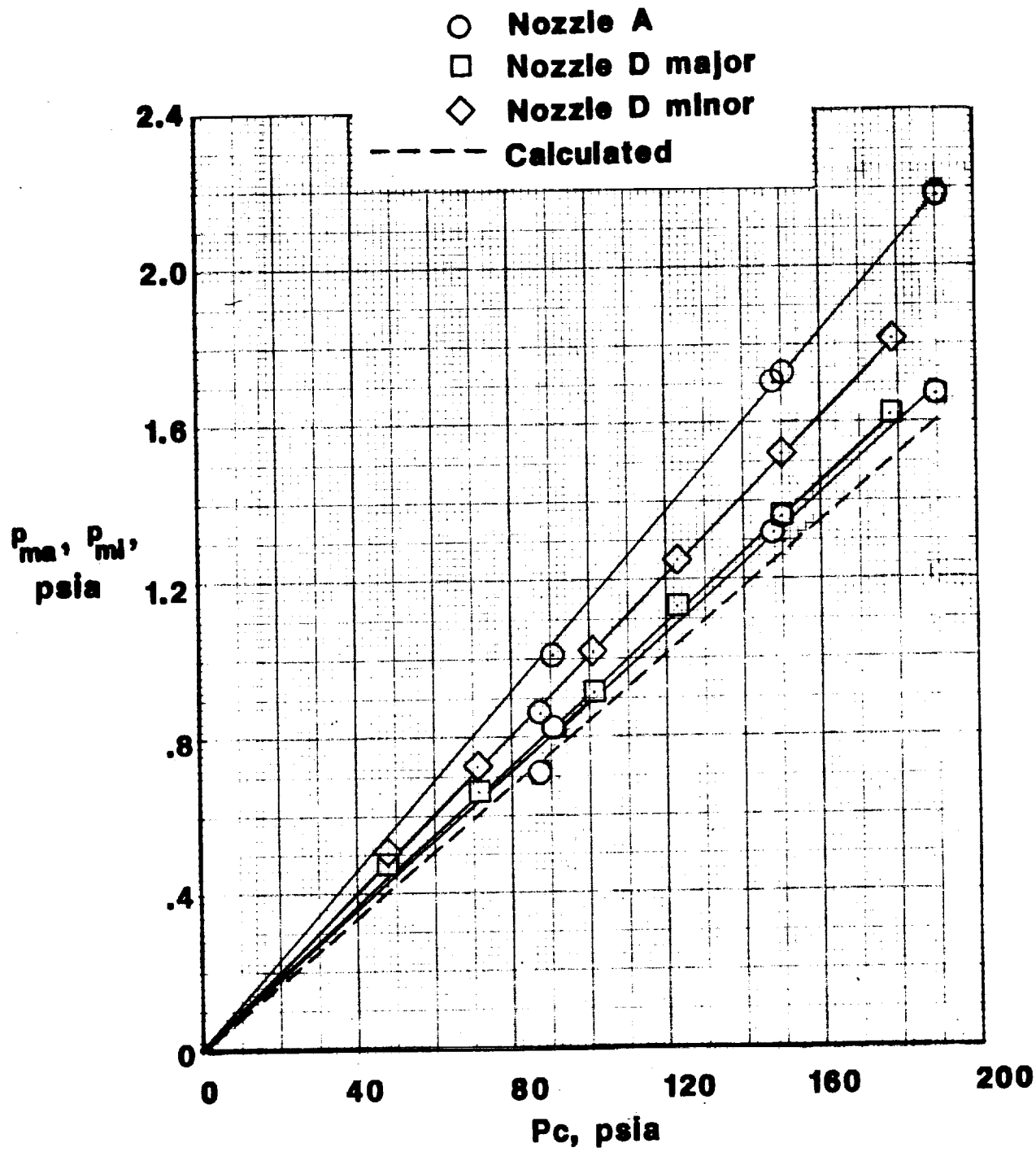

Figure 12.– Variation of pressure near the exit with chamber pressure for nozzles A and D.

NASA National Aeronautics and Space Administration

Report Documentation Page

1. Report No.	2. Government Accession No.	3. Recipient's Catalog No.
NASA TM-104097		

4. Title and Subtitle	5. Report Date
Effects of Nozzle Exit Geometry and Pressure Ratio on Plume Shape for Nozzles Exhausting into Quiescent Air	May 1991
	6. Performing Organization Code

7. Author(s)	8. Performing Organization Report No.
W. I. Scallion	
	10. Work Unit No.
	506-40-71-05

9. Performing Organization Name and Address	11. Contract or Grant No.
NASA Langley Research Center Hampton, VA 23665-5225	
	13. Type of Report and Period Covered
12. Sponsoring Agency Name and Address	Technical Memorandum
National Aeronautics and Space Administration Washington, DC 20546	14. Sponsoring Agency Code

15. Supplementary Notes

16. Abstract

The effects of varying the exit geometry on the plume shapes of supersonic nozzles exhausting into quiescent air at several exit-to-ambient pressure ratios are given. Four nozzles having circular throat sections and circular, elliptical and oval exit cross sections were tested and, the exit plume shapes are compared at the same exit-to-ambient pressure ratios. The resulting mass flows were calculated and are also presented.

17. Key Words (Suggested by Author(s))	18. Distribution Statement
Nozzle, Plume Shape, Exit Pressure Ratio Quiescent Air	Subject Category 02 Unclassified - Unlimited

19. Security Classif. (of this report)	20. Security Classif. (of this page)	21. No. of pages	22. Price
Unclassified	Unclassified	36	A03